

Viscoelasticity and Structures in Chemically and Physically Dual-Crosslinked Hydrogels: Insights from Rheology and Proton Multiple-Quantum NMR Spectroscopy

Xueting Zou,^a Xing Kui,^b Rongchun Zhang,^{c*} Yue Zhang,^b Xiaoliang Wang,^b Qiang Wu,^a Tiehong Chen,^{d,e} Pingchuan Sun,^{a,c,e*}

^a*Key Laboratory of Functional Polymer Materials of Ministry of Education and College of chemistry, Nankai University, Tianjin, 300071, P. R. China*

^b*Department of Polymer Science and Engineering, Nanjing University, Nanjing, 210093, China*

^c*State Key Laboratory of Medicinal Chemical Biology, Nankai University, Tianjin, 300071, P. R. China*

^d*Institute of New Catalytic Materials Science, School of Materials Science and Engineering, Key Laboratory of Advanced Energy Materials Chemistry (MOE), Nankai University, Tianjin, 300350, P. R. China*

^e*Collaborative Innovation Center of Chemical Science and Engineering (Tianjin), Tianjin, 300071, P. R. China*

*Corresponding Authors:

Rongchun Zhang, E-mail: zrcrong@nankai.edu.cn

Pingchuan Sun, E-mail: spclbh@nankai.edu.cn

The authors declare no competing financial interest.

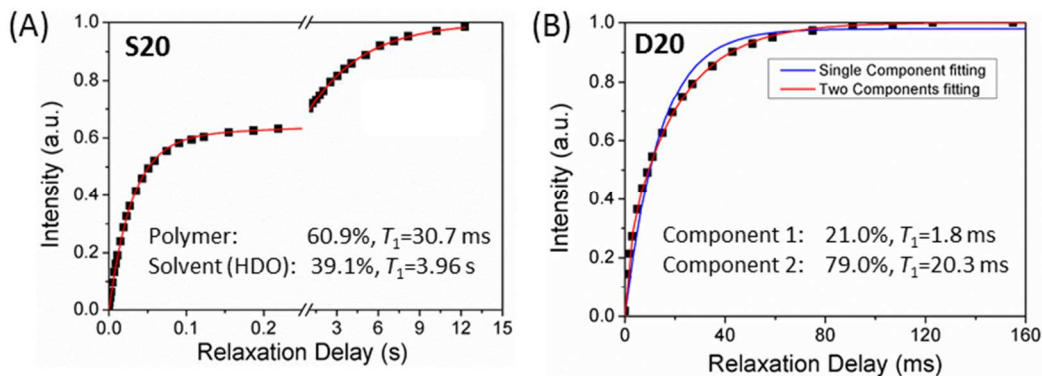


Figure S1. Buildup of the longitudinal magnetization for the S20 (A) and D20 (B) hydrogels measured by saturation recovery experiment with variable relaxation delay. The solid lines are the fitting results obtained with Eq. (1). As is clearly seen, in the S20 hydrogel, due to the large contrast in T_1 between polymer and solvent signals, their relative fraction in the hydrogel can be well determined. However, in the D20 hydrogel, due to the paramagnetic effects of Fe^{3+} ions, both T_1 of the polymer and solvent are dramatically reduced. In this case, although the longitudinal magnetization buildup curve still has to be fitted with two components, it is not clear whether these two components can be ascribed to solvent and polymer respectively. Besides, in the polymer, the protons close to Fe^{3+} and those far away from Fe^{3+} may have different T_1 , and the T_1 of the polymer protons far away from Fe^{3+} may be similar to the T_1 of solvent. As a result, the component with a large T_1 may contain the contributions of both the polymer and solvent.

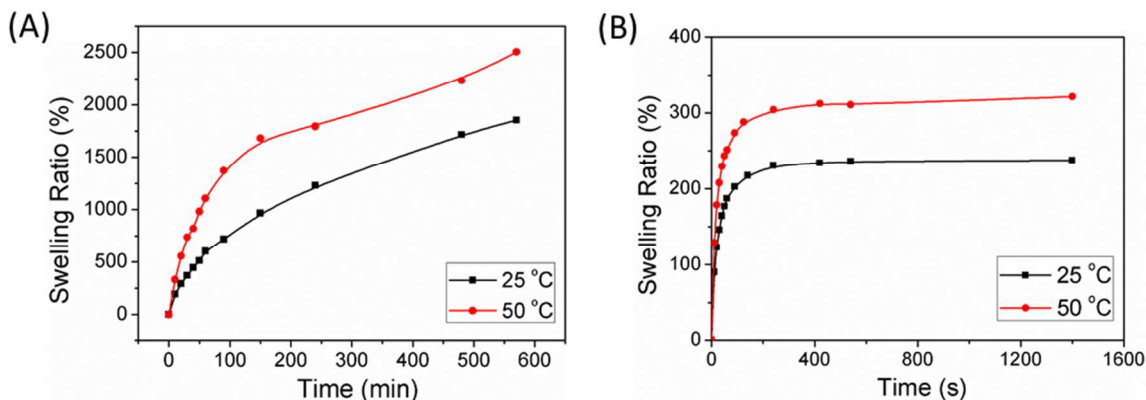


Figure S2. Swelling ratio as a function of the swelling time at a temperature of 25 and 50 °C for the S25 (A) and D25 (B) hydrogels. The swelling ratio was defined as $SR = (m_{\text{swollen}} - m_{\text{dry}}) / m_{\text{dry}} * 100\%$, where m_{swollen} and m_{dry} indicate the weight of the swollen and initial dried sample, respectively. As is clearly shown, the swelling capacity is enhanced at a higher temperature.

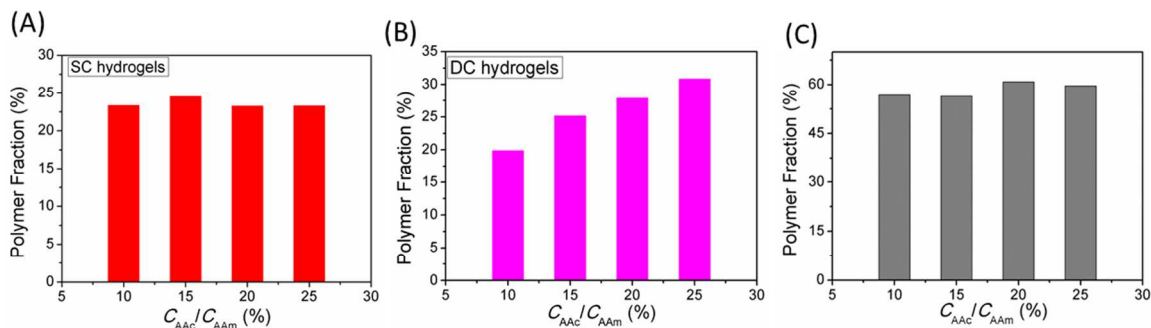


Figure S3. The weight fraction of polymers (m_{dry}/m_{wet}) in the SC (A) and DC (B) hydrogels with different C_{AAc}/C_{AAm} as determined by lyophilization. (C) The proton fraction of polymers in the SC hydrogel as a function of C_{AAc}/C_{AAm} as determined by the proton T_1 experiments as explained in the Experimental Section.

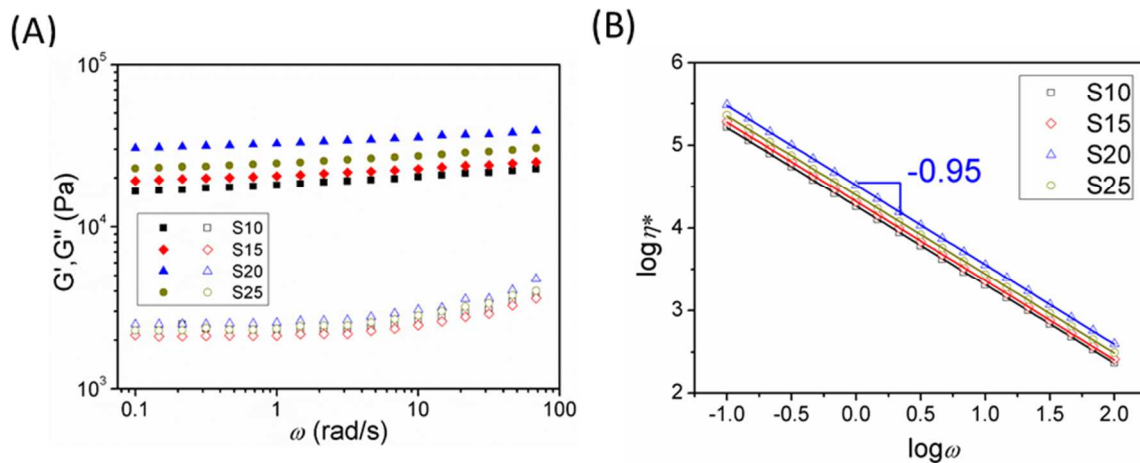


Figure S4. (A) Viscoelastic moduli (G' , G''), and (B) complex viscosity (η^*) as a function of the strain frequency for the SC hydrogels with a fixed C_{AAm} (3 mol/L) but varying C_{AAc} with a C_{AAc}/C_{AAm} of 10%, 15%, 20%, and 25%.

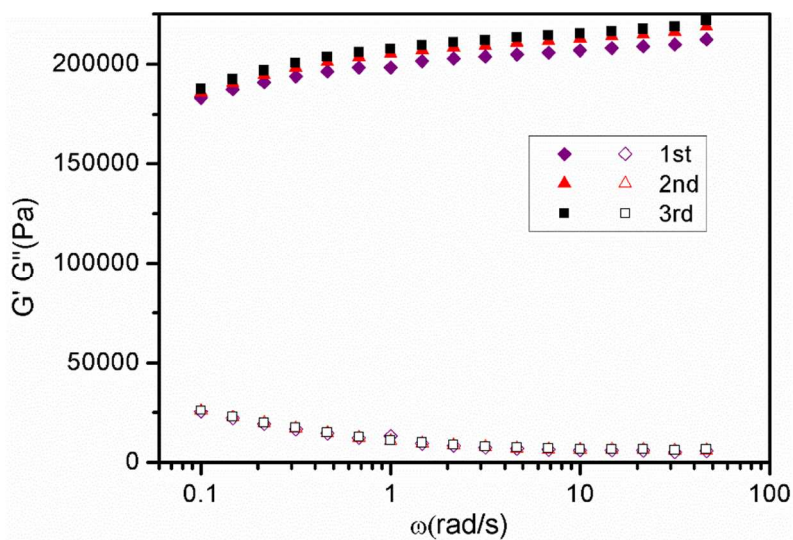


Figure S5. Viscoelastic moduli (G' , solid, G'' , open) as a function of the strain frequency for the D25 hydrogel in a repeated strain frequency sweep cycles. As is clearly shown, with increasing the strain frequency sweep cycles, the storage modulus G' gradually increases, especially when the strain frequency is large, demonstrating that the Fe^{3+} coordination complex with moderate/weak binding strength may transform to those with strong binding strength during the dynamic shear experiments.

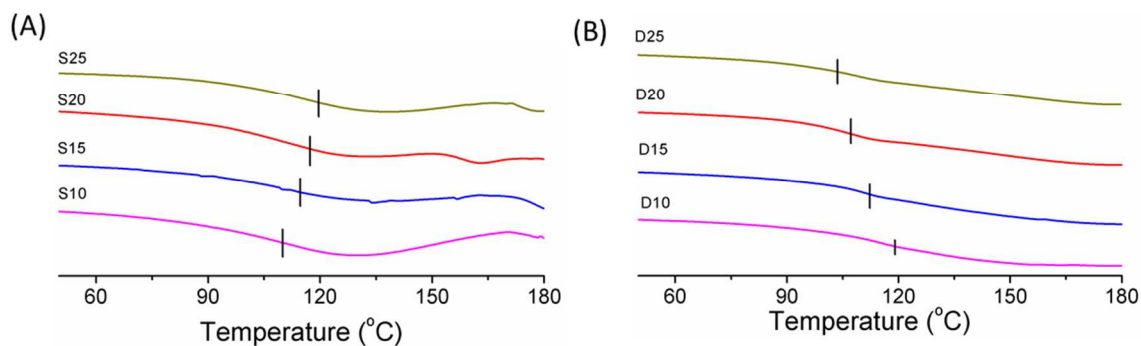


Figure S6. DSC traces of the SC (A) and DC (B) hydrogels. All the water in the hydrogels was removed by lyophilization before measurements. All the DSC measurements were performed on a Mettler-Toledo DSC1 differential scanning calorimeter under a nitrogen atmosphere with a heating rate of $10\text{ }^{\circ}\text{C}/\text{min}$. The T_g values were taken as the midpoints of the heat flow changes in the first heating scan.

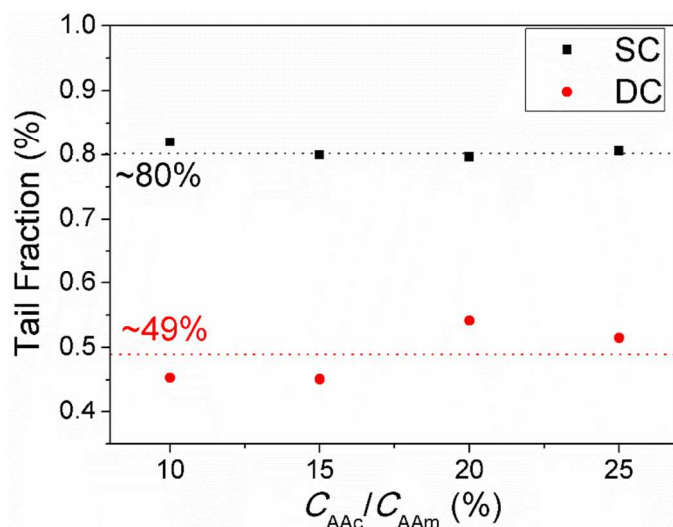


Figure S7. Tail fractions as obtained for SC and DC hydrogels from proton MQ NMR experiments. In all the proton MQ NMR experiments, recycle delay was set as 0.2s. Thus, for the SC hydrogels, all the solvent signals were filtered out. As a result, the tail fraction directly indicates *the fraction of the polymer defects with respect to the total polymer content*. However, for the DC hydrogels, the T_1 of solvent was quite short. Thus, the tail fraction indicates *the fraction of the polymer defects with respect to all the components in the hydrogel including solvents*.

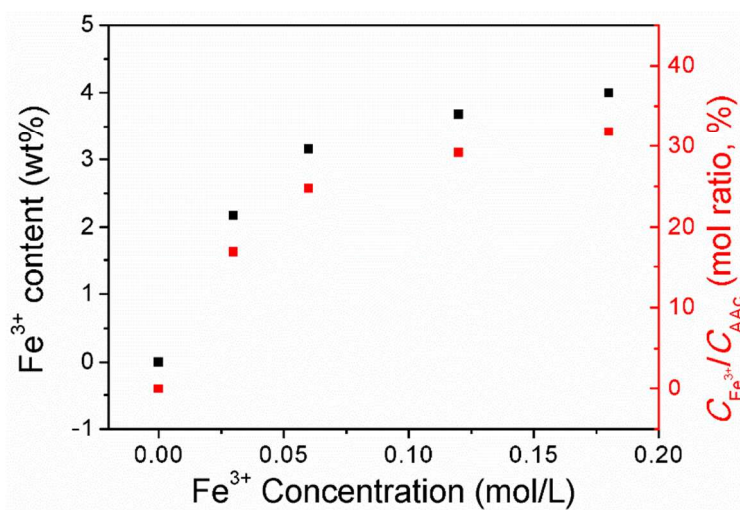


Figure S8. The final Fe^{3+} content in the D20 hydrogels prepared with different $FeCl_3$ concentration solution. (Left: weight ratio with respect to the dried hydrogel sample. Right: molar ratio with respect to the content of initial AAc monomers ignoring the influences of initiators and crosslinkers as well as the potentially unreacted AAc/AAM monomers in the sample) All the hydrogels were dried firstly, and then the weight ratio of Fe^{3+} were determined by inductively coupled plasma optical emission spectroscopy (ICP-OES) using a SPECTRO-BLUE instrument. Taking D20 hydrogel prepared with a 0.03 mol/L ferric solution as an example, where weight fraction of Fe^{3+} is $w(Fe)=2.17\%$ as determined by ICP-OES. Ignoring the small fraction of crosslinkers and initiators as well as the potential unreacted AAc/AAM monomers, the polymer fraction $w(\text{polymer})=1-2.17\%=97.83\%$. In the D20 hydrogels, the molar ratio C_{AAc}/C_{AAM} is 20%; therefore in the polymers, the weight fraction of AAc is $w(AAc)=0.2*72.06/(71.08*1+72.06*0.2)=16.85\%$. Herein, the molar ratio

$$\frac{C_{Fe^{3+}}}{C_{AAc}} = \frac{w(Fe)/56}{w(\text{polymer}) * 16.85\% / 72.06} = \frac{w(Fe)}{w(\text{polymer})} * 7.63 = 16.93\%$$

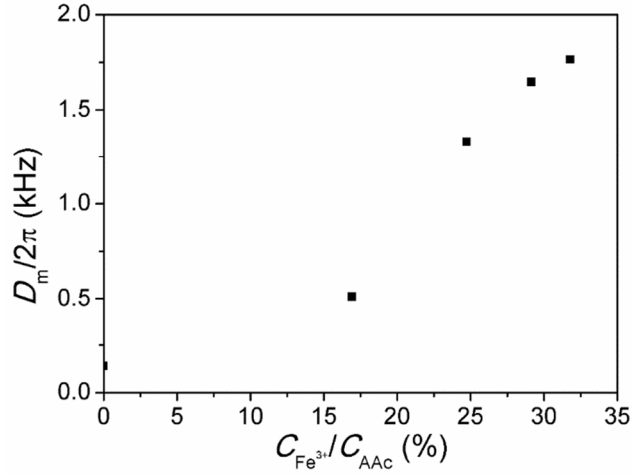


Figure S9. D_m as a function of $C_{Fe^{3+}}/C_{AAc}$ in the D20 hydrogels.

Comparison of the fraction of polymer defects in the hydrogels.

The fraction of polymer defects with respect to the total polymer content in the DC hydrogel can be obtained as

$$p_{defects}^{DC} = \frac{A_{defects}^{DC}}{A_{polymer}^{DC}} = \frac{A_{defects}^{SC} - A_{sol\ chains}^{SC} - A_{carboxylic\ acid\ groups}^{SC}}{A_{polymer}^{SC} - A_{sol\ chains}^{SC}} < \frac{A_{defects}^{SC} - A_{sol\ chains}^{SC}}{A_{polymer}^{SC} - A_{sol\ chains}^{SC}}$$

(S1)

$$\text{Let } a = \frac{A_{sol\ chains}^{SC}}{A_{defects}^{SC}}, \text{ and because } a < 1, p_{defects}^{SC} = \frac{A_{defects}^{SC}}{A_{polymer}^{SC}} < 1$$

$$\begin{aligned} \frac{A_{defects}^{SC} - A_{sol\ chains}^{SC}}{A_{polymer}^{SC} - A_{sol\ chains}^{SC}} &= \frac{A_{defects}^{SC} - aA_{defects}^{SC}}{A_{polymer}^{SC} - aA_{defects}^{SC}} = \frac{A_{defects}^{SC} - aA_{defects}^{SC}}{A_{polymer}^{SC} - ap_{defects}^{SC}A_{polymer}^{SC}} \\ &= \frac{A_{defects}^{SC}}{A_{polymer}^{SC}} \frac{1-a}{1-ap_{defects}^{SC}} < \frac{A_{defects}^{SC}}{A_{polymer}^{SC}} \end{aligned}$$

(S2)

$$\text{i.e. } p_{defects}^{DC} = \frac{A_{defects}^{DC}}{A_{polymer}^{DC}} < p_{defects}^{SC} = \frac{A_{defects}^{SC}}{A_{polymer}^{SC}} \quad (S3)$$